



# Employing MCNP to optimize experimental design for compressed sensing neutron source imaging<sup>☆</sup>



Nuraslinda Anuar<sup>a,b,\*</sup>, Craig Marianno<sup>a</sup>, Ryan G. McClarren<sup>c</sup>

<sup>a</sup> Department of Nuclear Engineering, Texas A&M University, College Station, TX 77843, United States

<sup>b</sup> Department of Mechanical Engineering, Universiti Tenaga Nasional, 43000 Kajang, Selangor, Malaysia

<sup>c</sup> Department of Aerospace and Mechanical Engineering, University of Notre Dame, Notre Dame, IN 46556, United States

## ARTICLE INFO

### Keywords:

Neutron source imaging  
Compressed sensing  
Compressive sensing  
Non-negative least squares

## ABSTRACT

Compressed sensing theory has been applied in the signal processing stage of many existing imaging systems. This research attempts to incorporate compressed sensing principles in conjunction with the collimator design. Monte Carlo N-Particle Transport Code (MCNP) was used to design a proof-of-concept experimental apparatus. This was accomplished by running simulations to determine: the height of water required to stop thermal neutrons from a <sup>252</sup>Cf source; collimator array dimensions; the collimator material; and the collimator size for the experiment. The simulations were run using a cylindrical water tank and a 2 × 2 array of channels acting as collimator. Three different materials were simulated to determine the best collimator composition for the experiment. An array configuration was defined as a random combination of air-filled and water-filled channels. Neutron counts were tallied using MCNP for each configuration with a total of 300 configurations for a 23 × 23 array and 100 for an 11 × 11 array. The image of the source corresponding to the different collimator array size was constructed using non-negative least squares with MATLAB. Another MCNP model with a rectangular tank was created with an 11 × 11 collimator array. Several images as a function of the number of measurements,  $K$ , were produced to observe the minimum  $K$  that would result in accurate image quality. These simulations have resulted in the decision to proceed with the assembly of an imaging system made of a water-filled 250-gallon tank with an array of 0.5-inch 11 × 11 polyvinyl chloride (PVC) pipes. The  $K$  required for a conventional raster scan method would be the total pixels, which is  $K = 121$  in the 11 × 11 case. It was found that the source shape and location can be obtained with  $K$  that is 50% of the total pixels.

## Contents

1. Introduction .....	1
2. Methodology .....	2
2.1. MCNP simulations .....	2
2.2. Image reconstruction .....	2
3. Results and discussions .....	3
4. Conclusion .....	4
Acknowledgments .....	5
References .....	5

## 1. Introduction

Traditionally, an image with  $M$  pixels requires  $M$  measurements to reproduce it and this method is known as the raster scan method [1]. Compressed (or compressive) sensing theory however allows for smaller

number of measurements,  $K$ , to recover information that was thought to be unrecoverable if  $K < M$  [2]. This information acquisition method has been utilized in signal processing and data storage applications, but very few studies have been performed in nuclear imaging applications [3–5]. A neutron imaging technique was proposed to include the principles of

<sup>☆</sup> Declarations of interest: none.

\* Corresponding author at: Department of Nuclear Engineering, Texas A&M University, College Station, TX 77843, United States.

E-mail address: [lynnanuar@tamu.edu](mailto:lynnanuar@tamu.edu) (N. Anuar).

URL: <https://nsspi.tamu.edu/> (N. Anuar).

compressed sensing in the collimator design [6]. It is emphasized that the objective of this research is to image a neutron source to determine its shape and size as this is useful for nuclear security applications.

This novel technique would be helpful in the efforts to monitor contraband nuclear materials transportation at shipping ports or land borders. Neutron source imaging may be better than just neutron detection as it would help in determining the level of response that is needed if the shape of the suspected neutron source could be visualized. One advantage of this design is that it allows for the use of only one or two neutron detectors to image a source with fast neutrons. The materials used for this proposed system design are also inexpensive and ubiquitous, making it inexpensive to acquire and implement. A system utilizing this technique could also be employed at nuclear installations to compare neutron image signatures for nuclear safeguards purpose.

The fundamental principle that allows for this technique to work is the fact that mathematically, signals obtained by measurements using compressed sensing can be translated into another set of signals that collectively form the image signals,  $x$ . Compressive sensing works because  $x$  is required to be  $s$ -sparse, which means that  $x$  can be represented using only  $s$  non-zero coefficients. As  $x$  is plotted as an image, lighter shades in  $x$  would represent the possible positions with stronger neutron intensity. Therefore, if a neutron source is present when the imaging takes place,  $x$  would be an  $s$ -sparse set of signals as it is expected that the neutron source is the dominant neutron emitter that would stand out from the surrounding.

The translation process utilizes incoherence of a sensing matrix,  $A$ , which maps  $x$  to the measured signals,  $b$ , the neutron counts. In linear algebra, coherence of a matrix is defined as the largest absolute normalized inner product between its different columns and this characterizes the dependence between the matrix columns. A small value of coherence (higher incoherence) would result in a better likelihood for successful signal recovery. To ensure incoherence, the sensing matrix is required to have randomness as a property. It is shown later in the methodology section that  $A$  is assigned to be a random combination of zeros and ones. Solving for  $x$  would eventually produce a 2D resemblance that identifies the shape and location of the imaged neutron source.

The image signals,  $x$ , are recovered using non-negative least squares (NNLS), in which a requirement for the sparse  $x$  entries to be non-negative is imposed [7,8]. Nonnegative entries are required because it is assumed that the image signals would consist of only positive values as they would indicate the presence of a neutron source. Other materials surrounding the source are not radioactive, and therefore will not generate positive values. Using the relation  $Ax = b$ ,  $x$  matrix recovery is achieved by using a built-in MATLAB function called *lsqnonneg* and is explained further in the methodology section. Monte Carlo N-Particle Transport Code (MCNP) [9] simulations were performed to determine the collimator array size (total pixels), dimensions and material for the experiment. Throughout this paper, the chronology of simulations that led to the final system design is elaborated and results are subsequently discussed.

## 2. Methodology

### 2.1. MCNP simulations

The preliminary simulations were based on a cylindrical water tank to determine the required water height to stop all thermal neutrons through scattering and absorption in water. A  $^{252}\text{Cf}$  isotropic point source was placed 50 cm above the water and a measurement surface for the  $F1$  tally was placed directly underneath the tank. The  $F1$  tally defined in MCNP measures particle current (neutron in this case) at an assigned surface. This means that neutron counts will be tallied whenever a neutron, regardless of its energy, crosses the surface of interest. Only direct streaming of neutrons from the source will be used for image reconstruction. Simulations with varying  $F1$  tally surface size

**Table 1**  
The dimensions of MCNP simulation models.

Item	Dimensions (cm)
Cylindrical tank	$31.48(R) \times 101(H)$
Parallelepiped tank	$101.6(W) \times 121.92(L) \times 137.16(H)$
23 × 23 pipe	$0.316(I D) \times 0.514(O D) \times 100(H)$
11 × 11 pipe	$0.635(I D) \times 0.912(O D) \times 100(H)$

were run to determine collimator dimensions that ensured minimal in-scatter from exterior neutrons.

The collimator was introduced vertically into the model at the tank's center as a 2 × 2 array. Simulations were run with three different types of collimator materials; stainless steel, polyvinyl chloride (PVC) and aluminum. Once the appropriate material was identified, an array size of 23 × 23 was arbitrarily chosen. A ring source was positioned at 50 cm above the water surface and was defined as a 1  $\mu\text{Ci}$   $^{252}\text{Cf}$  fission source emitting  $4.31 \times 10^3 \text{ ns}^{-1}$ . A ring source was chosen so that the image quality could be evaluated by the easiness of source shape and position identification. After the image produced using 23 × 23 array size was evaluated, the array size was reduced by half to see if there was any difference in the image quality. An acceptable image quality difference would mean that smaller array size may be employed as it would result in a more practical experiment. Another model with an 11 × 11 array size, but with a rectangular tank was simulated due to the availability of a rectangular tank for the experiment. The rectangular tank model used a 100  $\mu\text{Ci}$  of the same neutron source as one of the variance reduction methods in ensuring accurate MCNP results.

A configuration is defined as a combination of air-filled (empty) pipes and water-filled pipes. Empty pipes are represented as 1's in the  $A$  matrix while water-filled pipes are represented as 0's. This allows for neutron interactions to be defined as follows; the inner product of the  $A$  matrix with the image matrix,  $x$ , would then represent neutron absorption for multiplication with 0's and neutron streaming towards the  $F1$  tally surface at the end of the tank (where the detector will be in the experiment) for multiplication with 1's. The average open channel fraction of the collimator is 0.5. Three hundred random array configurations were created by a Python code for the 23 × 23 array and 100 configurations for the 11 × 11 array. This resulted in the creation of 300 and 100 MCNP input files for the 23 × 23 and 11 × 11 array, respectively. Each file was run, producing a corresponding output file that contains the  $F1$  tally results. These results form a  $b$  matrix that corresponds to the respective array size.

Table 1 shows the dimensions used in the MCNP models. The proposed neutron source imaging system is illustrated in Fig. 1. This diagram shows the cross sectional area of the proposed setup on the  $x$ - $z$  plane and the  $x$ - $y$  plane at  $z = 50$ , which is about halfway through the height of the tank. The collimator array is placed in the middle of the tank with rubber stoppers fixed at the bottom ends. Fig. 1 shows the configuration with all pipes filled with water (matrix  $A$  entries are all zeros). For proposed experiments, two  $^3\text{He}$  neutron detectors are placed beneath the tank and a neutron source is placed on or above the collimator. Depending on the row entries of matrix  $A$ , different configurations of collimator can be obtained by removing water (if the entry is 1) or adding water (if the entry is 0) into corresponding pipes.

### 2.2. Image reconstruction

A Python code was created to extract the array configurations from the MCNP input files and to rewrite in an Excel spreadsheet where each array configuration is stored as the row entry of the spreadsheet. The extracted data forms matrix  $A$ , which is therefore a  $300 \times 529$  matrix for the 23 × 23 array and  $100 \times 121$  for the 11 × 11 array. The  $F1$  tally results were also extracted from the corresponding output files and rewritten as the row entry in another spreadsheet. These entries in a new

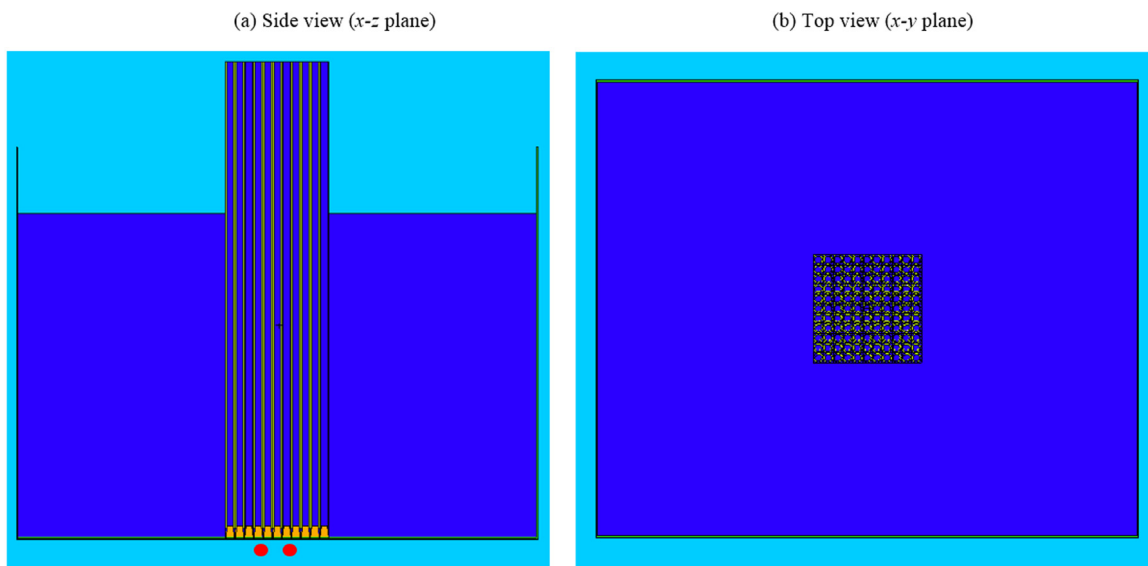


Fig. 1. Illustration of the proposed neutron source imaging system displayed using the MCNP Visual Editor software showing the cross-sectional views on the  $x-z$  plane at  $y = 0$ , and the  $x-y$  plane at  $z = 50$ .

Excel sheet makes matrix  $b$ . Here,  $b$  is a  $300 \times 1$  matrix for the  $23 \times 23$  array and  $100 \times 1$  for the  $11 \times 11$  array.

$$\min \|x\|_1 \text{ subject to } Ax = b \tag{1}$$

Image reconstruction in compressed sensing is usually solved using  $l_1$ -minimization. There are a few variations of  $l_1$ -minimization technique, depending on the type of problem to be solved. The earliest code was developed using MATLAB program and is known as the *l1-MAGIC* program [2]. An example of one way to solve for  $x = b/A$  by  $l_1$ -minimization is shown by Eq. (1), which is known as basis pursuit.

If a nonnegative vector,  $x$ , is recovered by  $l_1$ -minimization, then it is the unique nonnegative vector that satisfies  $Ax = b$ . Therefore,  $x$  can also be recovered by NNLS by solving for  $x = b/A$  and minimizing the  $l_2$  of the difference between  $b$  and the inner product of  $A$  and  $x$  as shown in Eq. (2). If the image,  $x$ , is nonnegative and sparse, the use of NNLS will typically solve for  $x$  if the NNLS uses the active Lawson–Hanson algorithm.

$$\min \|b - Ax\|_2 \text{ subject to } x \geq 0 \tag{2}$$

Solving for Eq. (2) using an active set is possible by solving an unconstrained least-square problem that includes only inactive variables, if the active variables are known [10]. This is done by attempting to find the nonnegative solution with some variables being assigned to zero. These variables are called an active set because of their non-negativity constraints being activated. The active set is modified by a single variable in each iteration and finally the unconstrained least-square problem is solved without the active set [11]. The *lsqnonneg* function in MATLAB executes the Lawson–Hanson algorithm that employs this active-set technique [8]. A comparison between the  $l_1$ -minimization solution and the NNLS solution is presented and discussed in the subsequent section for the  $23 \times 23$  array with the ring source positioned near the top-right corner of the collimator array with  $K = 300$ .

The recovered signal matrix,  $x$ , is shown as a gray-scaled image using the *imagesc* command in MATLAB. For the  $11 \times 11$  rectangular data, images were constructed with various numbers of measurements,  $K$ , starting from 100 and reduced to 30 with an interval of 10 measurements. The purpose of this was to observe the effect of  $K$  value on image quality.

### 3. Results and discussions

The initial simulations resulted in the requirement for a 100 cm height of water to stop all thermal neutrons (less than 0.025 eV) at the

bottom of the cylindrical water tank. This was reflected by the zero value of MCNP tally output for thermal neutrons. The array was required to be smaller than 25.3 cm by 25.3 cm to avoid in-scattering from the sides of the tank into the  $F1$  tally surface.

Placing a different material in the tank might cause some neutrons to reach the  $F1$  tally surface because of its lower neutron absorption cross section compared to that of water. Since most of the thermal neutrons are supposed to be absorbed by the determined water height, a material that would result in minimal number of neutrons to reach the  $F1$  tally surface would be preferable. Stainless steel was found to be the best collimator material as it caused minimal neutrons traveling through the length of the collimator compared to PVC and aluminum. However, there was only a  $0.17 \pm 0.09 \text{ ns}^{-1}$  average count rate increase when PVC was used as the collimator material. Since PVC pipes are less expensive than the stainless steel pipes, PVC was selected as the collimator material for the proof-of-concept experiment.

With these requirements, the neutron source image was reconstructed successfully by the  $23 \times 23$  array size using all measurements ( $K = 300$ ). The reduced array size to  $11 \times 11$  resulted in a source image with lower resolution as expected using all measurements ( $K = 100$ ), but with an image quality that still allows for source localization and shape identification. The reconstructed image,  $x$  using *l1-MAGIC* is compared with using *lsqnonneg* function in MATLAB in Fig. 2. It can be seen here that the NNLS technique gives the same solution as the  $l_1$ -minimization technique. Due to this similarity, all images in this work were then processed with the *lsqnonneg* function in MATLAB, with matrices  $A$  and  $b$  as its inputs. NNLS was chosen to solve for  $x$  because this technique is faster and readily available in MATLAB, while also producing a very similar solution as  $l_1$ -minimization solvers do.

A comparison between the images produced by the  $23 \times 23$  array and the  $11 \times 11$  array is shown in Fig. 3. It was determined that an  $11 \times 11$  would be a suitable and practical array size for a physical experiment. Due to availability of a rectangular 250-gallon water tank, another MCNP model with these new characteristics was built. The images produced as a function of  $K$  are depicted in Fig. 4 which shows that significant degradation of image quality was observed below  $K = 60$ . The source shape and location were changed to a larger ring placed in the middle of the collimator to facilitate better comparison of image quality as a function of  $K$ .

For measurements with low count rates, large relative error in  $b$  is expected. This will in turn result in large uncertainties in  $x$ . Ideally, the determination of the minimum  $K$  would be more precise by performing

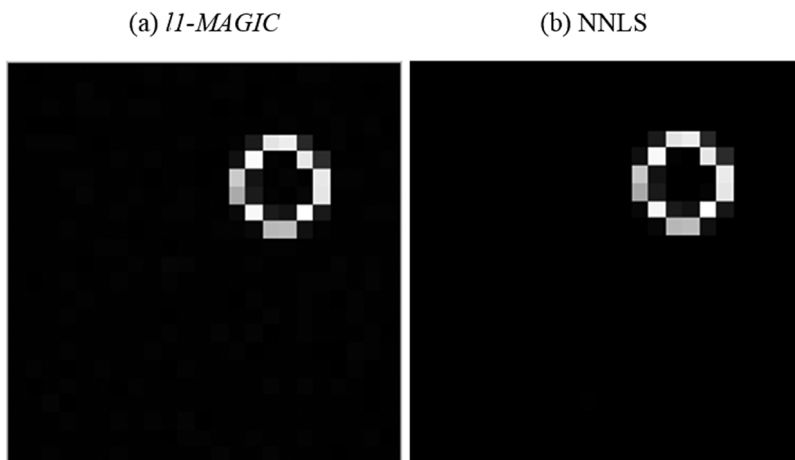


Fig. 2. Comparison between the solution produced by *l1-MAGIC* and *lsqnonneg* for a cylindrical tank with  $23 \times 23$  array for  $K = 300$ .

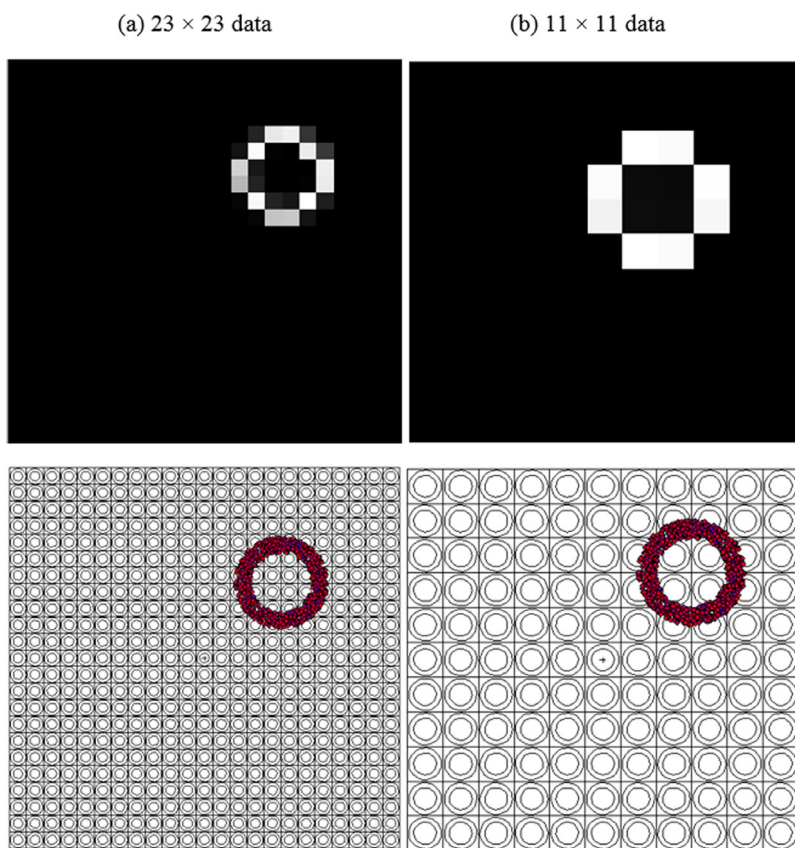


Fig. 3. The image produced using a cylindrical tank for a ring source at top-right corner by (a)  $23 \times 23$  simulation data with  $K = 300$ , and (b)  $11 \times 11$  simulation data with  $K = 100$ . The dotted plot depicting a ring in the bottom figures is the source plot displayed using the MCNP Visual Editor software with the top view of the array.

many reconstructions from multiple data sets (each data set contains measurements for 100 configurations). However, the simulations done so far are meant to serve as a benchmark for the actual experiment. For example, it should be possible to start seeing the source shape or location when at least  $K = 50$  measurements have been obtained. In the future, multiple data set reconstructions will be implemented for final design optimization.

MCNP simulations for this rectangular water tank show that for a ring source strength of  $100\mu\text{Ci}$  with  $^{252}\text{Cf}$  fission spectrum, the average total number of neutrons crossing the bottom of the tank for all of the configurations is  $2.58 \pm 1.6 \text{ ns}^{-1}$ . Assuming a neutron background of  $0.5 \text{ ns}^{-1}$  and a detector efficiency of 0.01, a 10-minute measurement for one

configuration would result in an expected average count of  $15.5 \pm 3.9$  and an expected background count  $3.0 \pm 1.7$ . These measurements are not statistically the same within  $2\sigma$  of each other, hence a 10-minute count (or longer) would be sufficient for analysis through the image reconstruction process.

#### 4. Conclusion

MCNP simulation results indicate that an  $11 \times 11$  array of PVC pipes would be sufficient and feasible to perform a physical experiment for neutron source image reconstruction. Simulations showed that image quality allowing for neutron source shape and location determination

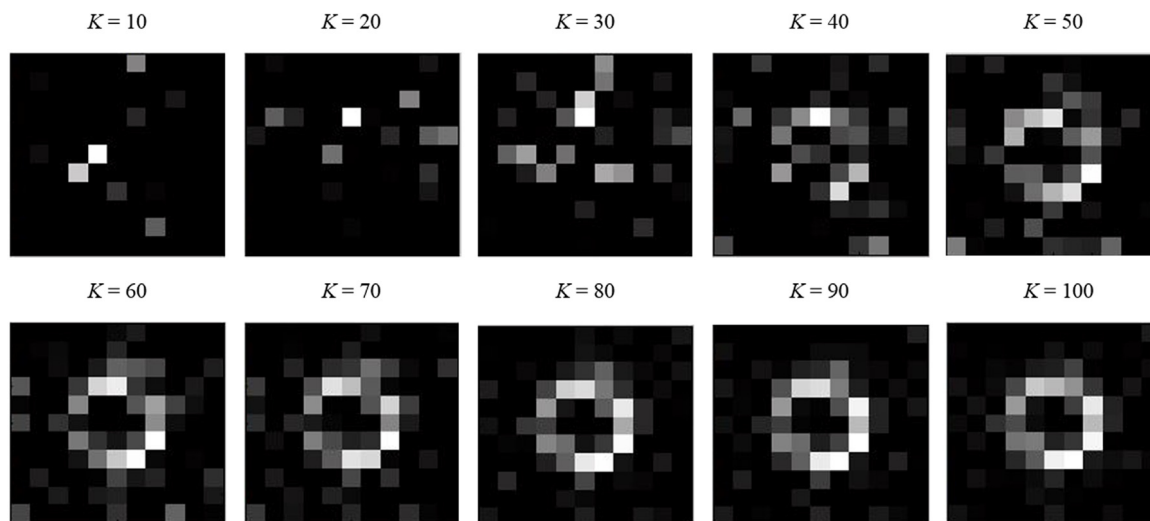


Fig. 4. Images produced at different  $K$  values for a simulation of a ring source at the center of a rectangular tank with an  $11 \times 11$  array.

is obtained with as low as 50% of the total pixels compared to the conventional raster scan method. This proves to be useful in realizing a system that is less expensive and more efficient in localizing and identifying the shape of a neutron source. This system is considered as inexpensive as it can only be built using water, PVC pipes, a water tank, and a water pumping system.

#### Acknowledgments

This research did not receive any specific grant from funding agencies in the public, commercial, or not-for-profit sectors.

#### References

- [1] W.S. Yeo, Raster scanning, Online, 2006. URL <https://ccrma.stanford.edu/~woony/research/raster/> (Accessed on 31.07.18).
- [2] E. Candes, J. Romberg, *l1-MAGIC: Recovery of Sparse Signals via Convex Programming*, *l1-MAGIC User Guide* (2005).
- [3] D. Vargas, R.C. Kurwitz, I. Carron, K.R. DePriest., Development of a neutron spectroscopic system utilizing compressed sensing measurements, *EPJ Web Conf.* 106 (2016) <http://dx.doi.org/10.1051/epjconf/201610607002>.
- [4] W. Jin, Z. Liu, G. Li., Block-based compressed sensing for neutron radiation image using WDFB, *Adv. OptoElectron.* (2015) <http://dx.doi.org/10.1155/2015/496863>.
- [5] B. Gestner, Compressive sensing for nuclear security, Tech. rep., Sandia National Laboratory (2013).
- [6] Y.J. Ayzman, *Single Pixel Neutron Camera Using Compressive Sensing*, (Master's thesis), Texas A&M University, 2015.
- [7] P.D. O'Grady, S.T. Rickard, Compressive sampling of non-negative signals, in: *IEEE Workshop on Machine Learning for Signal Processing*, 2008, pp. 133–138.
- [8] S. Foucart, D. Koslicki, Sparse recovery by means of nonnegative least squares, *IEEE Signal Process. Lett.* 21 (4) (2014).
- [9] T. Goorley, M. James, T. Booth, F. Brown, J. Bull, L. Cox, et al., Initial MCNP6 release overview, *Nucl. Technol.* 180 (3) (2012) 298–315.
- [10] J. Chen, C. Richard, J.C.M. Bermudez, P. Honeine, Nonnegative least mean square algorithm, *IEEE Trans. Signal Process.* 59 (2011).
- [11] TNT-NN: A fast active set method for solving large non-negative least squares problems. *Procedia Comput. Sci.*, 2017, 108, 755–764, <https://doi.org/10.1016/j.procs.2017.05.194>.